2.4 Measurements at AUG

2.4.1 AUG July/August 1999 (30 keV pure He-beam)

Our first He beam emission measurements were parasitic. As described in chapter 2.1 a pure He beam at half the nominal energy was injected at the end of the heating beam injection for 200 ms. The conversion of one PINI to He operation was possible for an experimental program with low NBI power needs. This was the case for the investigation of neo-classical tearing-modes (NTMs) where pulses with only 3 MW NBI heating power were used.

The CER diagnostic was needed for the ion temperature measurements. However, not all of its fibres (viewing lines) are used by the spectrometer, therefore it was possible to connect four CER-fibres to a spectrometer from the Li-beam (LIB) diagnostics which remains unused for normal operation. For about 20 pulses He was injected, and the LIB spectrometer was set to the wavelength of one of the $n = 3 \rightarrow 2$ or $n = 4 \rightarrow 2$ HeI transitions for each pulse. In that way the 11 most intensive visible HeI lines [29] were covered, but no HeI beam emission signal could be identified.

Unfortunately, it was discovered later that the image amplifier has not been working, and the sensitivity of the CCD sensor on its own was not high enough to resolve the beam emission signal.

For some repetitive pulses it was not necessary to measure the ion temperature for each pulse, therefore the CER diagnostic could be used to measure the HeI beam emission. In that way the beam emission profile of three HeI lines (see Tab. V) could be measured with the CER spectrometer. These results were presented in [29].

AUG pulse	wavelength [nm]	HeI transition	beam energy [keV]	equi. beam current [A]	maximum intensity of beam emission
12635	502 nm	2^1S-3^1P	27 keV	14.2 A	1.7 e19 ph/m³s
12643	587.6 nm	2^3P-3^3D	27 keV	14.2 A	50.0 e19 ph/m³s
12644	667.8 nm	2^1P-3^1D	27 keV	14.2 A	4.0 e19 ph/m³s

Tab. Fehler! Verweisquelle konnte nicht gefunden werden.**: Observed HeI transitions, beam parameters, and maximum intensity of the beam emission profiles for three successful pulses of the first campaign at AUG.**

The intensity of the Doppler-shifted beam emission was weak and the resulting emission profile had a large scatter. As for the viewing lines close to the plasma edge the Doppler-shift was too small, the beam emission peak could not be separated from the unshifted passive emission from the edge. Therefore the plasma edge was outside the accessible radial region, and it was also not possible to identify the beam emission as an increase of the total emission (shifted plus unshifted).

2.4.2 AUG Mai 2000 (60 keV doped He/D-beam)

After the first campaign at AUG (chapter 2.4.1) successful measurements with a He/D-doping system have been made at JET (chapter 2.5.1). Consequently a similar system has been installed at AUG in April 2000. Between 25/4/2000 and 8/6/2000 the new system was tested and HeI beam emission measurements have been carried out.

The He/D doping system can be used for parasitic measurements without restrictions to the NBI heating power. By installing the doping system at the ion source Q3 the accessible radial range could be extended (details see chapter 2.1).

For the beam emission measurements the CER spectrometer was needed, therefore only pulses where the ion temperature measurements have not been needed could be used for our parasitic experiments. Furthermore, we were interested in a series or repetitive pulses, in order to obtain a set of comparable beam emission profiles. The ideal candidate meeting these requirements was the standard H-mode pulse.

Standard H-mode discharge

The AUG standard H-mode pulse is routinely performed during the start-up sequence of AUG. It is well characterised and the measurement of the ion temperature is not necessary. Fig. 2.23 shows the time trace of some important signals of the standard H-mode discharge #13665.

AUG pulse number	**13646**	**13665**	**13667**	**13782**	**time [s]**
stored energy [MJ]	0.589	0.594	0.625	0.562	3.5
heating power [MW]	4.88	4.87	4.88	4.94	3.5
density [10^{19} 1/m^3]	*6.29*	5.13	5.27	5.12	3.5
stored energy [MJ]	0.567	0.537	0.56	0.558	6.3
heating power [MW]	4.76	4.86	4.84	4.85	6.3
density [10^{19} 1/m^3]	*12.5*	10.26	10.32	10.38	6.3

Table VI: Reproducibility of the AUG standard H-mode pulse at low density.

The two flat top phases, one with a line average density of $5 \cdot 10^{19}$ m^{-3} between 2.5 and 4.5 s, and another one with a line average density of 10^{20} m^{-3} between 5.5 and 7 s, had been used for the HeI beam emission measurements. The stored energy of the AUG plasma is roughly the same in both periods, which means that the electron temperature is correspondingly lower in the high density phase of the discharge. Helium gas for producing a doped He/D beam was injected into the ion source between 3.5 and 3.7 s and between 6.1 and 6.3 s. The reproducibility of the discharges was very good with only one pulse (#13646) showing a 20 % higher density in table VI. The standard H-mode pulse was used for measuring the beam emission of all visible He lines which were accessible (the spectrometer could not be set to wavelengths above 7000 Å).

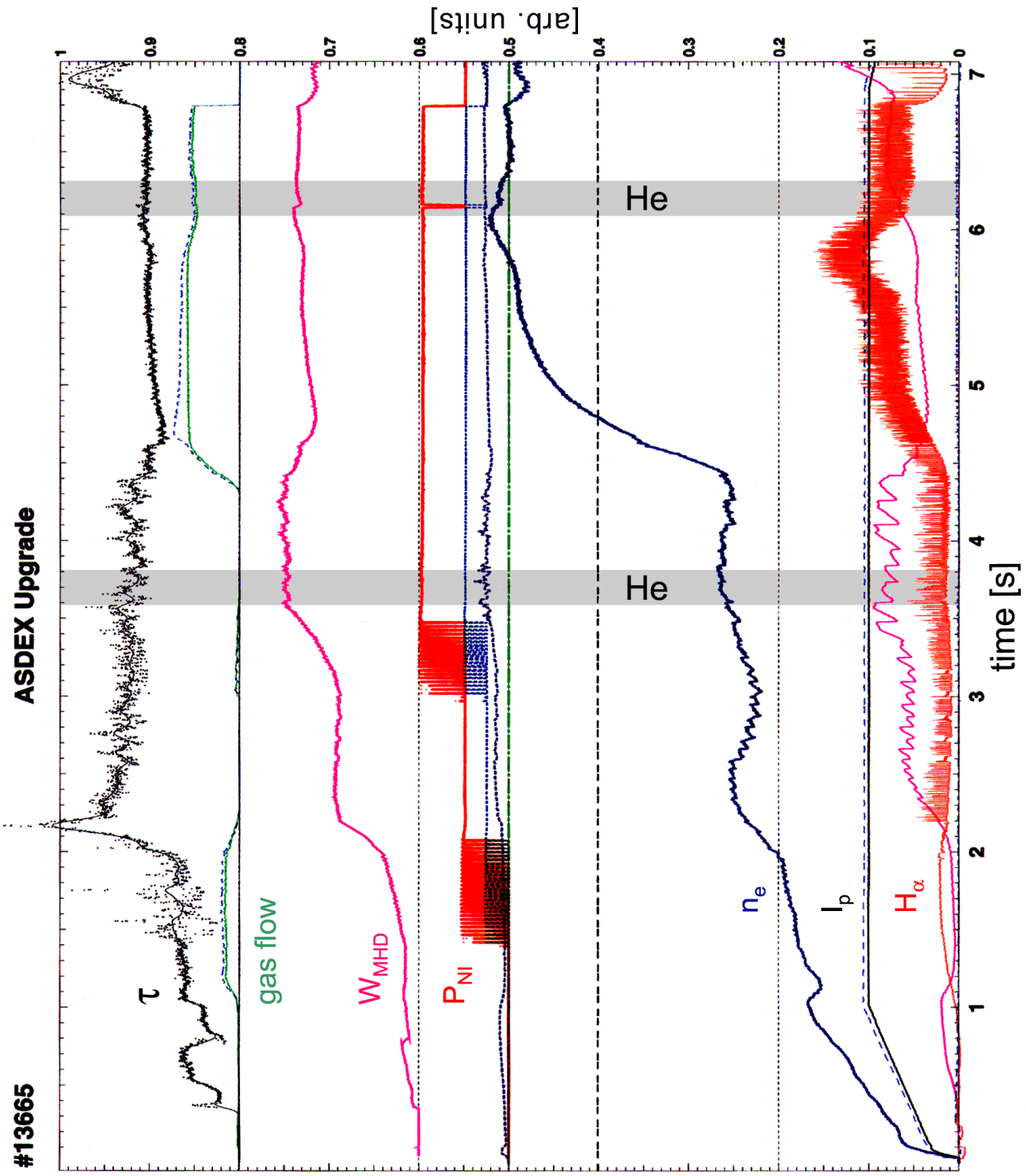

Fig. 2.23: Plasma parameters of the AUG standard H-mode discharge #13665. He doping, marked by grey bars, was performed at 3.5 and 6.1 s. The transition into H-mode at t = 2 s is characterised by an increase in confinement (stored energy W_{MHD}, confinement time τ, and electron density n_e).

Other abbreviations: P_{NI} ....injected neutral beam power
I_p .....plasma current
H_α ....passive plasma H_α-emission (ELM-activity).

The ramp-up of the plasma current up to Ip = 1 MA occurs during the first second of the discharge (ohmic phase). Subsequently the NBI heating power is being ramped up between 1.4 and 2.1 s to about 3.75 MW (on/off modulation). At t = 2.2 s the transition into the H-mode occurs. This can be seen from the significant increase of the energy confinement time τ from 0.06 to 0.13 s and the increase of the stored energy up to W_{MHD} = 0.36 MJ. The plasma density (electron density n_e) increases as well, although the gas flow decreases at the same time, indicating an increased particle confinement. For a short time after the L-H-transition the energy confinement time goes up to τ = 0.2 s, and is lost again shortly thereafter with the first ELM-event. The ELMs (edge localised modes) can be identified from the H_α-signal (Balmer-alpha line at 656 nm), which increases during an ELM-event when the unstable plasma edge collapses.

During the first flat-top phase (t = 2.5 - 4.5 s) the average plasma density settles at $n_e = 5 \cdot 10^{19}\ m^{-3}$. This means that during this phase the density is above the set-point and only defined by the gas flux from the wall. From t = 3 to 3.5 s the beam power is ramped-up to 7 MW.

After the second power ramp-up the first He injection into the ion source was triggered.

After t = 4.4 s the control parameter for the plasma density is doubled ($n_e = 1 \cdot 10^{20}\ m^{-3}$). This can also be seen in the gas flow. At about t = 5.5 s the density of the second flat-top phase is reached and kept constant till t = 7 s.

Other discharges at AUG

Emission from the strongest He lines could also be measured in two other discharges that are characterised in table VII.

pulse & number		time [s]	stored energy [MJ]	heating power [MW]	density [1/m^3]
Killer pellet	#13647 / 8	2.5	0.476	4.99	$5.09 \cdot 10^{19}$
ITB	#13742 / 3	1.6	0.64	5.38	$4.18 \cdot 10^{19}$

Table VII: Main plasma parameters of two further AUG pulses with He beam emission data

The "killer pellet pulse" is a pulse driven towards a high-density disruption and then terminated by a killer pellet. The increase of the density starts at 2.9 s, termination with the pellet occurs shortly before 6 seconds. Helium for the doped beam was injected into the ion source before the density rise at 2.5 s. At his time the discharge is a flat-top H-mode discharge without additional gas fuelling and consequently very similar in density to the first phase of the standard H-mode pulse.

The second pulse type was a so-called ITB discharge. A characteristics for this type of discharge is that additional heating is already supplied during the current rise phase. At the time of the He injection (1.6 s) there is no additional gas fuelling. The density is lower than in the case of the standard H-mode pulse, while the stored energy is higher.

Density profiles

Density profiles can be obtained from different diagnostics. The signal "DCN+Li" from the ddf-database is a combination of the profile obtained from several laser channels of the Interferometry (DCN) and the profile delivered by the Li beam diagnostics (limited to the scrape-off layer). The profile is smoothed and regarded as most reliable. Thomson scattering and reflectometry are other diagnostics yielding density profiles. Not all diagnostics are available for every pulse and the range of some diagnostics can be limited. For some pulses the Thomson scattering system was moved to view the divertor and was therefore not available for evaluation of the core plasma.

The density profile can normally be well presented by

$$n(\rho) = n_0 \times (1+\alpha\rho^2) \times \begin{cases} 1 & \text{for } \rho < \rho_s \\ \left(1 - e^{-\frac{\rho-\rho_s}{\lambda}}\right) & \text{for } \rho \geq \rho_s \end{cases} \qquad \begin{array}{l} \rho \text{ .... normalised flux radius} \\ \rho_s \text{ .... radial position of step in profile} \end{array} \tag{3}$$

as Fig. 2.24 shows by using interferometric data.

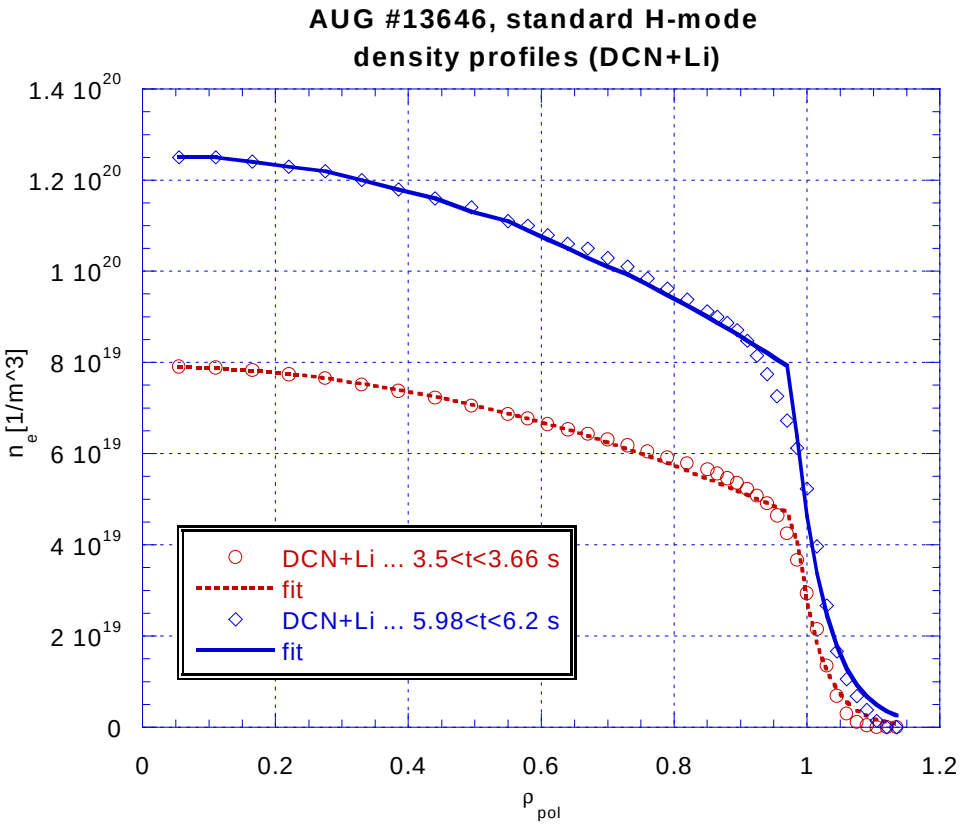

Fig. 2.24: AUG standard H-mode. Density profiles at 3.6 and 6 s taken from DCN and Li beam diagnostics at time intervals with He doped beam.

Temperature profiles

At AUG the main diagnostics for electron temperature profiles are Thomson scattering and the ECE radiometer. From Thomson scattering also a fitted profile called "Thomson fit" is stored in the AUG ddf database. When available, the "Thomson fit" data is being used for the temperature profile. For pulses without Thomson fit data the ECE radiometer data looks most promising, although its scatter can be considerable.

Fig. 2.25 shows the electron temperature profile for the standard H-mode pulse #13665 as derived from Thomson scattering data.

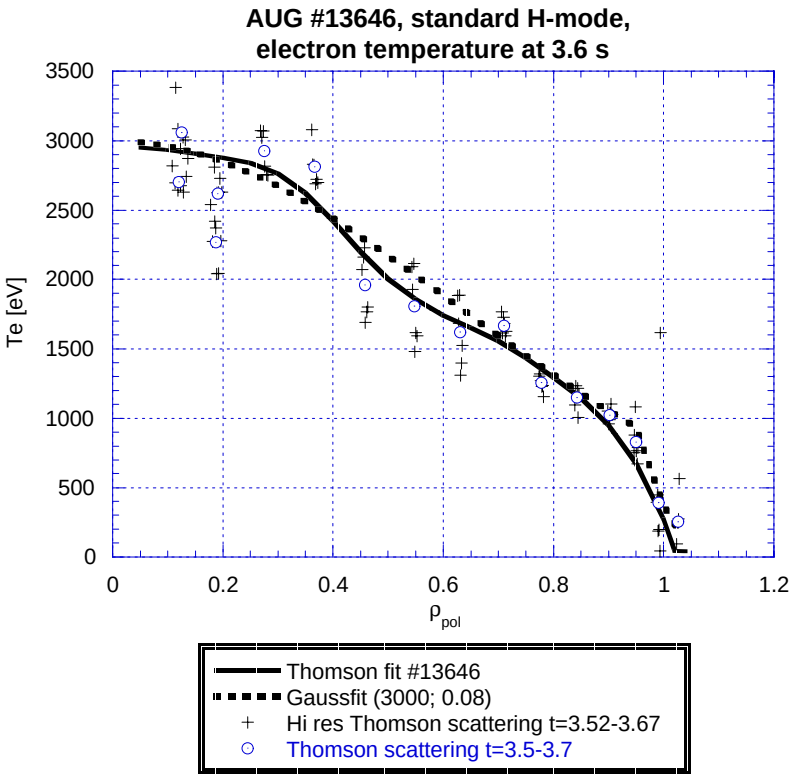

Fig. 2.25: Electron temperature profile for the standard H-mode discharge #13646 at t = 3.6 s. Symbols are straight data from Thomson scattering (standard and high resolution), the fit is from the standard Thomson scattering. Data points and Thomson fit show a centrally peaked profile. However, also a Gauß fit is consistent with the data due to its large scatter.

HeI beam emission for the standard H-mode discharge

The straight HeI beam emission profiles show a high systematic scatter. As described in chapter 3.6, this can be explained by the alignment of the CER diagnostic to the beam and is being corrected. Even for the most intensive singlet line the signal intensity was close to the noise level, leading to a considerable scatter in the beam emission profile. For evaluation of the HeI spectra we used the standard CER fitting routine (`cer_wid`), which was not optimised for our requirements.

Figs. 2.26 and 2.27 show the corrected beam emission profiles for the most intensive singlet (2^1P-3^1D) and triplet (2^3P-3^3D) line measured during the low density phase of standard H-mode discharges. In order to obtain a smoother profile, an average over 3 measurements from 3 equivalent discharges has been made as shown in Fig 2.26.

The singlet beam emission measurement can be reproduced by the model calculations if an initial population of the metastable 2^1S state of 1% is assumed. For these model calculations `scotty_fwd` was used, with n_e and T_e from Fig. 2.24 and 2.25 mapped onto the He beam axis.

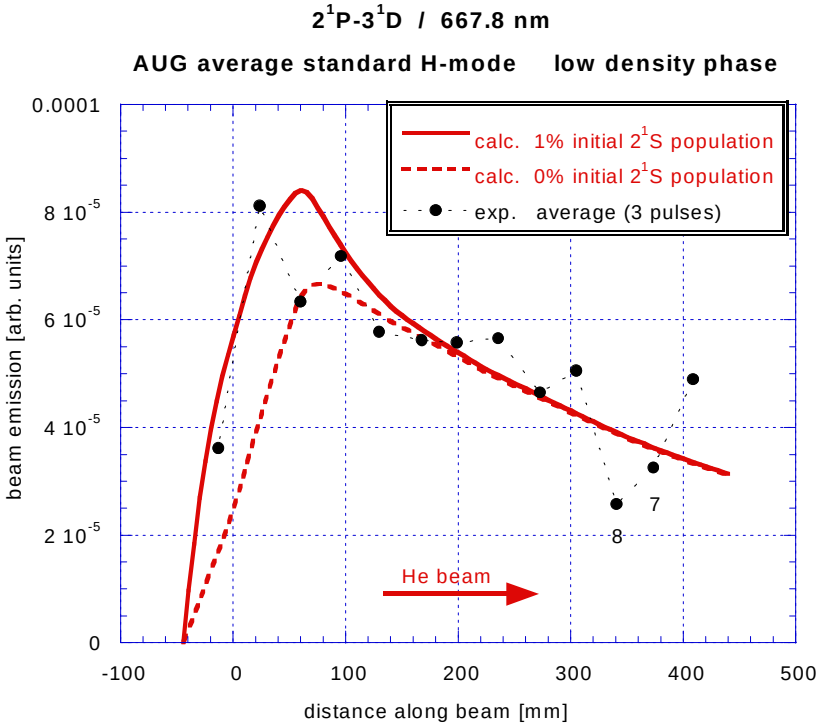

Fig. 2.26: He beam emission measurements (average over AUG #13646, #13667, #13880) and modelling of the HeI transition 2^1P-3^1D (667.8 nm). The measurements can be reproduced by the model calculations if an initial population of the 2^1S state of 1% is assumed.

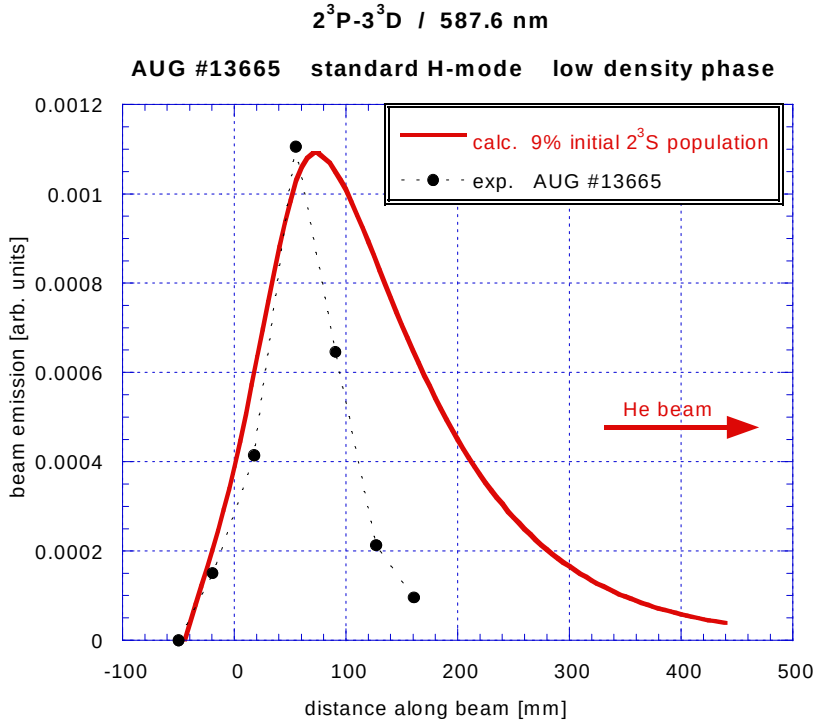

Fig. 2.27: Beam emission measurement and modelling of the HeI transition 2^3P-3^3D (587.6 nm) for the AUG discharge #13665. The obvious discrepancy in the curve width is discussed in chapter 2.6.3.

The two points labelled in Fig. 2.26 with their fibre numbers 7 and 8 show a clear tendency of too low values for different discharges and wavelengths. See also Fig. 3.12 in chapter 3.6. This could be due to calibration errors for these channels.

In Fig 2.27 an obvious discrepancy between the curve width of the measured and the calculated profile can be seen. This problem is discussed in chapter 2.6.3.

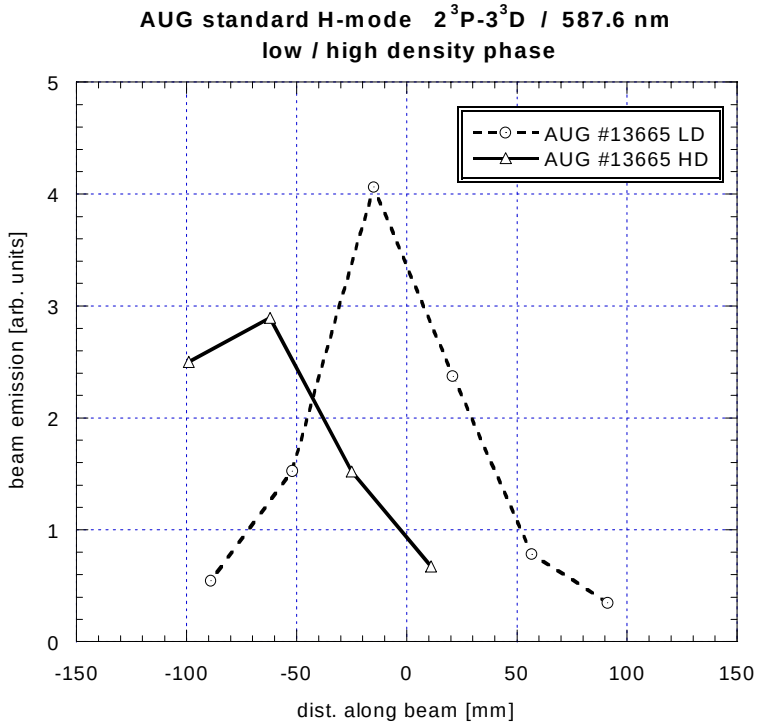

Fig. 2.28: Comparison of the triplet HeI beam emission (2^3P-3^3D) for low and high density phase.

The profiles measured during the high density phase are shifted relative to the profiles measured during the low density phase by about 40 to 50 mm. In Fig 2.28 the triplet emission profiles from the low and the high density phase are plotted in the same graph. The abscissa is defined as the distance along the beam, where the position of the LCFS defines zero. For the high density case the position of the maximum emission appears to be moved outwards beyond the LCFS and only the decaying part of the emission profile is within the range of the CER lines-of-sight. In the low density case (Fig. 2.26 and 2.27) the position of the steep increase of the emission profile is in agreement with the model calculations. For the high density case the modelled emission profiles need to be shifted outwards to match the measurement. In the plot of Fig 2.29 good agreement between the measured data and the model calculation could be achieved with a shift of 40 mm. This shift could be explained by a mapping error (EFIT) or by an error in the density profile used for the modelling.

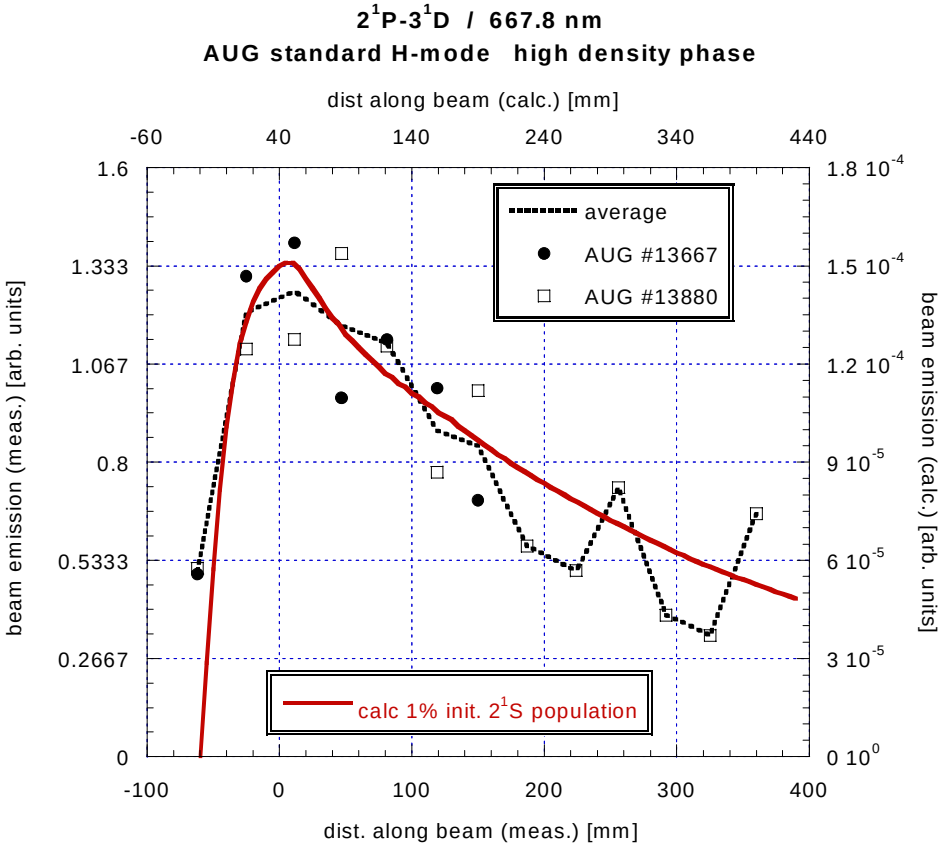

Fig. 2.29: Beam emission measurements (AUG #13667, #13880, and average) and modelling of the HeI line (2^1P-3^1D). The two abscissas (meas. and calc.) were shifted against each other by 40 mm.

2.4.3 Conclusions from Experiments at AUG

The generation of a fast He beam at AUG was achieved for both pure and doped D/He beams. The doped D/He beam had the advantage that the diagnostic PINI could be used for it, which provided a better viewing geometry giving access to a wider radial range. Another advantage was that the timing of the He doping is freely selectable and that the available NBI power stays unchanged. This gives access to relevant phases of a plasma discharge, whereas experiments using the pure He beam had to be scheduled at the end of the heating period.

Such beam emission experiments could be carried out parasitically with the only restriction that the CER diagnostic is not available for the ion standard temperature measurement.

The HeI lines 2^1P-3^1S, 2^3P-3^3S, and 2^3S-3^3P were not accessible due to technical limitations of the spectrometer. With regard to the other $n = 3 \rightarrow 2$ and $n = 4 \rightarrow 2$ HeI transitions, the sensitivity of the CER spectrometer was only high enough for the two strongest lines (transition 2^1P-3^1D at 667.8 nm and 2^3P-3^3D at 587.6 nm). For these two accessible lines we obtained beam emission profile for 4 different discharges and made repetitive measurements which allowed to estimate the error in the data to ±10%. This relatively high scatter is due to the low intensity of the signal. A systematic deviation of some channels indicates their non-perfect calibration.

The alignment of the beam to the CER viewing-lines was unfavourable and made an intensity correction of the different channels necessary. In particular, the outer lines-of-sight are very sensitive to misalignment. Furthermore, the intensity of the observed signal is lower.

The triplet emission was only measurable over the outer 200 mm of the plasma. This range is only roughly twice the range of the 50 kV lithium beam.

Since our last measurements the alignment and calibration of the CER diagnostic has been improved, which should lead to a higher beam emission signal and a lower scatter of the derived emission profile. The settings of the spectrometer (slit-width and exposure time) can be optimised in view to the signal intensity.

At JET a cross-calibration of neighbouring channels could be achieved by sweeping the plasma across the viewing-lines (see chapter 2.3.2). The application of this procedure to AUG is being investigated and would improve the achievable profile quality.